

Calculation of cross sections for vibrational excitation and dissociative attachment in electron collisions with HBr and DBr

Jiří Horáček

*Department of Theoretical Physics, Faculty of Mathematics and Physics,
Charles University Prague, V Holešovičkách 2, 180 00 Praha 8, Czech Republic*

Wolfgang Domcke

Institute of Physical and Theoretical Chemistry, Technical University Munich, D-85748 Garching, Germany

(Received 22 June 1995)

The nonlocal resonance model developed earlier for the description of low-energy inelastic and reactive electron-HCl collisions has been adapted to the electron-HBr collision system. The parameters of the model have been determined by fitting the eigenphase sum in the fixed-nuclei approximation to the data of an *ab initio* *R*-matrix calculation of Morgan, Burke, and collaborators. The Schwinger-Lanczos method has been employed to solve the nuclear scattering problem with a nonlocal, complex, and energy-dependent effective potential. Fully converged cross sections have been obtained on a dense grid of energies for many vibrational excitation, deexcitation, and dissociative channels in both HBr and DBr. The computed cross sections are generally in good agreement with experiment as far as data are available.

PACS number(s): 34.80.-i, 34.80.Ht

I. INTRODUCTION

The collision of low-energy electrons with hydrogen halide molecules is a surprisingly involved process and continues to represent a challenge for electron-molecule collision theory despite 20 years of research. The complexity of the problem arises from the intricate interplay of shape resonance effects, which efficiently couple the electron scattering dynamics with the vibrational motion, with effects of the long-range dipole potential, which couples the electronic motion with nuclear rotations and causes a dramatic enhancement of threshold structures. Since the discovery of threshold peaks in vibrational-excitation (VE) functions [1,2] and pronounced cusp structures in the dissociative attachment (DA) cross sections [3] of HF and HCl, these unusual threshold phenomena have been investigated in considerable detail both experimentally and theoretically. Cross sections for VE and DA in HX gases ($X = \text{F, Cl, Br, I}$) are required for the modeling of laser plasma and are, therefore, also of considerable applied interest [4,5].

The VE cross sections in HF do not show a discernible shape resonance, but exhibit pronounced threshold phenomena [1,2,6–8]. In HCl, the shape resonance is clearly developed and reflected by a broad peak near 3 eV in the VE cross sections [1,2,6–9]. In HBr, the shape resonance is even more pronounced than in HCl and located at lower energy (≈ 1 eV) [10]. The intensity of the threshold peaks relative to the shape resonance feature decreases from HF to HBr, which seems to reflect the decrease of the dipole momentum [1,2,10]. The unusual threshold phenomena observed in electron collision with HF and HCl have stimulated extensive theoretical work. The threshold peaks in $e + \text{HF}$ VE functions have been explained by vibrational or rovibrational close-coupling treatments based on *ab initio* *R*-matrix calculations [11–13]. For the $e + \text{HCl}$ collision system the so-called nonlocal resonance model, which can be derived either from the Feshbach projection-operator formalism [14] or the *R*-matrix

formalism [15], has provided a rather detailed description of resonance and threshold features in VE and DA cross sections [16–18]. An alternative model is the effective-range model of Teillet-Billy and Gauyacq [19]. *Ab initio* scattering calculations of the *R*-matrix type, combined with the nonadiabatic treatment of the vibrational motion, also have produced VE cross sections for HCl in good agreement with experiment [20]. For a more complete account of the extensive literature, we refer to recent review articles [15,21–23].

Only very few theoretical studies have been concerned with the electron-HBr collision system. The most comprehensive theoretical investigation to date has been performed by Morgan, Burke, and collaborators using the *ab initio* *R*-matrix approach [24]. Based on the fixed-nuclei scattering calculations including polarization effects, elastic electron scattering cross sections and VE functions have been obtained [24]. It seems that the DA process in HBr has not theoretically been treated so far.

In the present work we adapt the nonlocal resonance model to the electron-HBr collision system. In the nonlocal resonance model, the $^2\Sigma$ low-energy shape resonance accounts for the coupling of the electron scattering dynamics with the vibrational motion, while the threshold effects caused by the long-range dipole potential are included via a threshold expansion of the energy-dependent width function [23,25]. As in previous applications, the rotational dynamics of the target molecule is neglected in the present work. This should be a good approximation except for electron energies within a few meV of the threshold [11]. The parameters of the model are determined via a least-squares fit of the fixed-nuclei eigenphase sum as a function of energy and internuclear distance to the *ab initio* data of Fandreyer *et al.* [24]. In addition, information on the bound-state potential-energy function of HBr^- at large internuclear distances obtained by large-scale multiconfiguration self-consistent-field (MCSCF) and configuration-interaction (CI) calculations [26] is taken into account.

The calculation of cross sections within the nonlocal resonance approach requires the solution of the Lippmann-Schwinger (LS) equation involving energy-dependent, complex, and nonlocal effective potentials. This technical problem was solved by Mündel and Domcke [27] employing separable expansions of the nonlocal potentials. This approach made use of analytic solutions (Green's functions and scattering states) of Morse potentials and is therefore not immediately applicable for general potentials. Pless *et al.* [28] have more recently developed a fully numerical and thus generally applicable method. Alternatively, a time-dependent approach has been implemented by Gertitschke and Domcke which is suitable for arbitrary potential functions [18]. Here we discuss the implementation of yet another generally applicable method, the Schwinger-Lanczos (SL) approach [29–31]. This iterative approach seems to be well suited to treat scattering problems with complicated nonlocal potential operators. We develop in the present work a modification of the Schwinger-Lanczos approach which renders the computation considerably more efficient. With this method, fully converged VE excitation cross sections for many channels and DA cross sections for various initial vibrational levels have been obtained for both HBr and DBr. We report here the most interesting data, hoping that this may stimulate further experimental investigation of this little studied collision system. Preliminary results of the present investigation have been reported in [32].

II. OUTLINE OF THE THEORY

The present modeling of resonance and threshold effects in electron-HBr collision closely follows the approach developed earlier for the electron-HCl system [17]. Therefore only a brief outline of the general theoretical framework will be given here. A more comprehensive exposition of the theory can be found in [23].

The formulation is based on the projection-operator approach of scattering theory [14] which provides a well-established framework for the description of resonances in electron-molecule scattering [23,33–37]. We assume that the electronic Hilbert space is spanned by a single discrete electronic state (which represents the $^2\Sigma^+$ shape resonance for short internuclear distances and the $^2\Sigma^+$ bound state of HBr⁻ for large internuclear distances) and a single orthogonal continuum. Assuming the diabaticity [38] of these electronic states and projecting the time-independent Schrödinger equation on the discrete subspace, one obtains an effective equation describing nuclear dynamics in an energy-dependent, complex, and nonlocal potential. Denoting by $V_0(R)$ and $V_d(R)$ the potential-energy (PE) functions of the target molecule and the discrete state, respectively, and by $V_{d,k}$ the discrete-continuum coupling matrix element, the effective potential reads [23]

$$V_{\text{eff}}(R, R'; E) = V_d(R) \delta(R - R') + F(R, R'; E), \quad (1)$$

$$F(R, R'; E) = \Delta(R, R'; E) - \frac{i}{2} \Gamma(R, R'; E), \quad (2)$$

$$\Delta(R, R'; E) = \sum_v \int dE' V_{d,E'}(R) \chi_v(R) [E - E' - \epsilon_v]^{-1} \chi_v^*(R') V_{d,E'}^*(R'), \quad (3)$$

$$\Gamma(R, R'; E) = 2\pi \sum_v \int V_{d,E-\epsilon_v}(R) \chi_v(R) \chi_v^*(R') V_{d,E-\epsilon_v}^*(R'). \quad (4)$$

The $\chi_v(R)$ are eigenstates of the target vibrational Hamiltonian

$$H_0 = T_N + V_0(R), \quad (5)$$

$$T_N = -\frac{\hbar^2}{2\mu} \frac{d^2}{dR^2}, \quad (6)$$

with eigenvalues ϵ_v . In Eqs. (3) and (4) we have introduced an angle-averaged discrete-continuum matrix element which is defined via

$$|V_{d,E}|^2 = \int d\Omega_k |V_{d,k}|^2. \quad (7)$$

In order to compute cross sections for VE and DA, we have to solve the Lippmann-Schwinger equations [23]

$$|\psi_{d,E}^{(+)}\rangle = G_0^{(+)} V_{d,k_i} |v_i\rangle + G_0^{(+)} (V_d + F) |\psi_{d,E}^{(+)}\rangle \quad (8)$$

and

$$|K^{(+)}\rangle = |K\rangle + G_0^{(+)} (V_d + F) |K^{(+)}\rangle. \quad (9)$$

Here $|K\rangle$ denotes a state of free radial nuclear motion and $G_0^{(+)}$ is the resolvent operator for the free radial nuclear motion

$$G_0^{(+)} = (E - T_N + i\eta)^{-1}, \quad (10)$$

η being the usual positive infinitesimal. $|\psi_{d,E}^{(+)}\rangle$ and $|K^{(+)}\rangle$ are scattering states in the effective potential V_{eff} with boundary conditions appropriate for electron scattering and DA, respectively.

In the actual calculations it is convenient to absorb the strong, but local, part $V_d(R)$ of the effective potential into the unperturbed problem. Applying the well-known two-potential formula, Eqs. (8) and (9) are rewritten as

$$|\psi_{d,E}^{(+)}\rangle = G_d^{(+)} V_{d,k_i} |v_i\rangle + G_d^{(+)} F |\psi_{d,E}^{(+)}\rangle \quad (11)$$

and

$$|K^{(+)}\rangle = |K_d\rangle + G_d^{(+)} F |K^{(+)}\rangle, \quad (12)$$

where

$$G_d^{(+)} = (E - T_N - V_d + i\eta)^{-1} \quad (13)$$

and $|K_d\rangle$ is a scattering state in the potential $V_d(R)$.

The integral cross sections for electron scattering and DA are given by

$$\sigma_{v_f v_i}(E) = \frac{4\pi^3}{k_i^2} |\langle v_f | V_{dE_f}^* | \psi_{d,E_i}^{(+)} \rangle|^2 \quad (14)$$

and

$$\sigma_{\text{DA}}(E) = \frac{4\pi^3}{k_i^2} |\langle v_i | V_{d,E_i} | K^{(+)} \rangle|^2. \quad (15)$$

III. CONSTRUCTION OF A MODEL FOR HBr

In the treatment of the theory outlined above, the collision system is characterized by three functions, namely, (i) the PE function $V_0(R)$ of the target molecule, (ii) the PE function $V_d(R)$ of the discrete state, and (iii) the discrete-continuum coupling element $V_{d,E}(R)$, or equivalently, the width function

$$\Gamma(R, E) = 2\pi |V_{d,E}|^2. \quad (16)$$

For the PE function of the $X^1\Sigma^+$ state of HBr we adopt a Morse potential

$$V_0(R) = D_0(e^{-2\alpha_0(R-R_0)} - 2e^{-\alpha_0(R-R_0)}), \quad (17)$$

and the parameters D_0 and α_0 are obtained by fitting spectroscopic constants [39] ($D_0 = 3.92$ eV, $\alpha_0 = 0.96$ a.u.⁻¹) and $R_0 = 2.67$ a.u., $\mu = 0.99558$ amu. The specification of the two other functions, $V_d(R)$ and $\Gamma(R, E)$, is much more difficult. Both functions can in principle be obtained from an *ab initio* calculation. Such calculations, though possible on current computers, are very involved and have been performed only for the simplest systems. To our knowledge there exists no calculation of the width function $\Gamma(R, E)$ for HBr⁻. We can use, however, existing *ab initio* data for elastic scattering in the fixed-nuclei approximation to infer the required parameters. This can be done as follows [17]: The eigenphase sum in the vicinity of a resonance can be decomposed into a background and a resonant part

$$\delta_{\text{sum}}(E, R) = \delta_{\text{bg}}(E, R) + \delta_{\text{res}}(E, R), \quad (18)$$

where the background term δ_{bg} is assumed to be a smooth function of E and R and all the rapid changes are concentrated in the resonance term δ_{res} , which is given by the Breit-Wigner formula with energy-dependent width and level shift [17,25]

$$\delta_{\text{res}}(R, E) = -\tan^{-1} \left(\frac{\frac{1}{2}\Gamma(R, E)}{E - V_d(R) + V_0(R) - \Delta(R, E)} \right). \quad (19)$$

Recently, Fandreyer *et al.* [24] have calculated the eigenphase sum $\delta_{\text{sum}}(R, E)$ for a range of R (2.0 a.u. < R < 3.1 a.u.) and $E < 0.8$ Ry. By fitting these data the unknown functions $V_d(R)$ and $\Gamma(R, E)$ can be obtained. As soon as the width $\Gamma(R, E)$ is known, the level shift $\Delta(R, E)$ can be calculated as

$$\Delta(R, E) = \frac{1}{2\pi} P \int_0^\infty \frac{\Gamma(R, E')}{E - E'} dE'. \quad (20)$$

To perform the fit of the data we must specify analytic expressions for the functions to be fitted. First we assume that the background term δ_{bg} is R independent and can be described in accordance with the threshold law as [38,40]

$$\delta_{\text{bg}}(E) = (\pi/4 - \alpha\pi/2) + aE^\alpha + bE. \quad (21)$$

Here $\alpha = 0.424$ is the threshold exponent [38] corresponding to the dipole momentum of HBr ($D = 0.828$ D) [41]. After some experimentation we found that the most stable fit is obtained when the discrete state potential $V_d(R)$ is taken in the form of a single exponential

$$V_d(R) = D_1 e^{-2\alpha_1(R-R_0)} + Q_1. \quad (22)$$

The quantity Q_1 is related to the electron affinity of Br [42] and for HBr we have $Q_1 = 0.56$ eV. It remains to specify the width function $\Gamma(R, E)$. Following the earlier proposal by Domcke and Mündel [17] we parametrize this function as

$$\Gamma(R, E) = \Gamma(E)g(R)^2, \quad (23)$$

with

$$\Gamma(E) = A(E/B)^\alpha e^{-E/B} \quad (24)$$

and

$$g(R) = e^{-C(R-R_0)}. \quad (25)$$

Altogether we have seven parameters to be determined: two background phase-shift parameters (a and b), two parameters describing the discrete state potential $V_d(R)$ (D_1 and α_1), and three parameters A , B , C describing the width function $\Gamma(R, E)$. The seven parameters have been determined by a least-squares fit of $\delta_{\text{sum}}(R, E)$ to the *ab initio* $^2\Sigma^+$ eigenphase sum of [24]. The quality of the fit can be deduced from Fig. 1 showing the *ab initio* data [24] in the range $0 < E < 4$ eV and $2.5 < R < 2.9$ a.u. In the figure the crosses are the *ab initio* data of Fandreyer *et al.*; the solid lines represent our fit, the dashed line corresponds to the equilibrium distance 2.67 a.u. The deduced values of the model parameters are $D_1 = 1.736$ eV, $\alpha_1 = 0.9871$ a.u.⁻¹, $A = 4.039$ eV, $B = 4.615$ eV, and $C = 0.1176$ a.u.⁻¹.

Although the effect of the polarization potential on the threshold expansion of $\Gamma(E)$ and $\delta_{\text{bg}}(E)$ has not been taken into account in Eqs. (21) and (24), the effect of the polarizability of HBr is included in the parameters determined by fitting the *ab initio* eigenphase sum obtained in the static-exchange-polarization approximation [24]. The fact that the $^2\Sigma^+$ shape resonance is located at lower energy and is narrower than the resonance in $e + \text{HCl}$ can to a large extent be attributed to the larger polarizability of HBr.

To check the reliability of our model we performed a series of fits in which the *ab initio* data were modified by an additional "noise." It was observed that the parameters A , B , D_1 , and α_1 are very stable with respect to changes of the amplitude of the noise. The parameter C describing the R dependence of the width function $\Gamma(R, E)$ is, however, sensitive to minor changes of the data. The value of C is thus not very accurately determined by the available *ab initio* data.

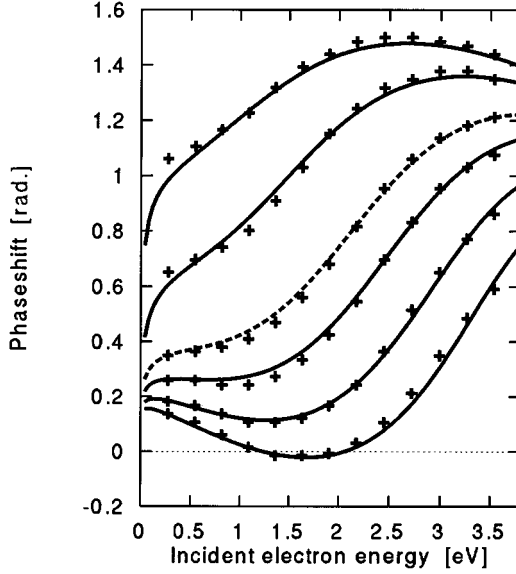


FIG. 1. The ${}^2\Sigma^+$ eigenphase sum for fixed-nuclei electron HBr scattering for the internuclear distances 2.4, 2.5, 2.6, 2.67, 2.8, and 2.9 a.u. (from bottom to top). Crosses are the *ab initio* data of Fandreyer *et al.* [24]. The solid lines show the eigenphase sum of the present model, the dashed line corresponds to the equilibrium distance 2.67 a.u.

Our calculations of VE cross section (see below) have shown, moreover, that the height and the width of the threshold peak in the $v=0\rightarrow 1$ channel depend very sensitively on the potential-energy function of HBr^- at large internuclear distances. The available *ab initio* electron-HBr scattering data [24], extending only up to $R=3.1$ a.u., are not sufficient to determine the HBr^- potential-energy function over the relevant range of R . To improve the model, we have modified the R dependence of the width function outside the range covered by the *ab initio* calculations of Ref. [24] as follows: for $R>R_1$

$$g(R) = e^{-C(R-R_0)} e^{-D(R-R_1)}. \quad (26)$$

The parameters R_1 and D have been adjusted in order to optimize the agreement of the bound-state potential-energy function of the model with the *ab initio* MCSCF-CI potential-energy function of Chapman *et al.* [26], resulting in $R_1=2.9$ a.u. and $D=0.4$ a.u. $^{-1}$.

The PE curves of the model are shown in Fig. 2. The dashed curve represents the ${}^1\Sigma^+$ ground-state potential energy of HBr, the dash-dotted curve the PE function of the ${}^2\Sigma^+$ discrete state of HBr^- . The full curve represents the adiabatic potential-energy function of the ${}^2\Sigma^+$ shape resonance ($R\leq 3$ a.u.) and the ${}^2\Sigma^+$ bound state of HBr^- ($R\geq 3$ a.u.), respectively. The cusp near 3 a.u. arises from the effect of the long-range dipole potential, see [23] for a detailed discussion. The bound-state part of the HBr^- potential-energy function exhibits a shallow minimum near $R=4.5$ a.u., in agreement with the *ab initio* MCSCF-CI potential-energy curve of Chapman *et al.* [26].

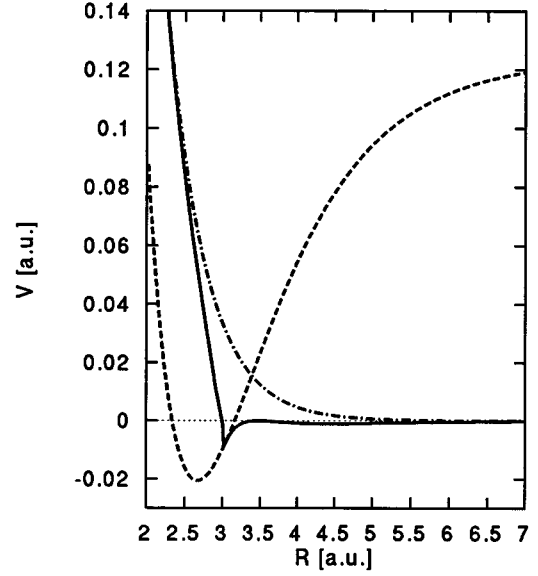


FIG. 2. Potential-energy curves of the model. The dashed curve represents the ${}^1\Sigma^+$ ground-state potential energy of HBr, the dash-dotted curve the potential-energy function of the ${}^2\Sigma^+$ discrete state of HBr^- . The full curve represents the adiabatic potential-energy function of the ${}^2\Sigma^+$ shape resonance ($R\leq 3$ a.u.) and the ${}^2\Sigma^+$ bound state of HBr^- ($R\geq 3$ a.u.), respectively.

IV. THE SCHWINGER-LANCZOS METHOD

To calculate VE and DA cross sections, the LS equation (8) or (9) must be solved. The potential operator F in these equations is nonlocal, complex, and energy dependent, see Eqs. (2)–(4). In some cases it is possible to approximate F by a local complex potential [35,43,44]. It is well known, however, that the nonlocality of F is absolutely essential for a correct description of the threshold peaks [17,25]. There exist several methods of solving Eqs. (8) and (9) with different degrees of generality [16,23,28]. Here we use the Schwinger-Lanczos method [29–31] which represents a fairly general and very efficient method of solving the LS equation.

Let us formally write the LS equation as

$$|\varphi\rangle = |u\rangle + G_d F |\varphi\rangle. \quad (27)$$

According to the SL method we define a set of states $\{|g_i\rangle\}$ as

$$|g_1\rangle = |u\rangle \langle u|F|u\rangle^{-\frac{1}{2}}, \quad (28)$$

$$\beta_i |g_{i+1}\rangle = G_d F |g_i\rangle - \alpha_i |g_i\rangle - \beta_{i-1} |g_{i-1}\rangle, \quad (29)$$

which diagonalize F and tridiagonalize $FG_d F$,

$$\langle g_i | F | g_j \rangle = \delta_{i,j}, \quad (30)$$

$$\langle g_i | F G_d F | g_{i-1} \rangle = \beta_{i-1}, \quad (31)$$

$$\langle g_i | F G_d F | g_i \rangle = \alpha_i, \quad (32)$$

$$\langle g_i | F G_d F | g_{i+1} \rangle = \beta_i, \quad (33)$$

$$\langle g_i | F G_d F | g_j \rangle = 0, \quad |j-i| > 1. \quad (34)$$

In the above equations $|u\rangle$ is the unperturbed wave function, G_d is the Green's function in the absence of F , and F is the nonlocal interaction. Once the vectors $|g_i\rangle$ have been constructed the solution $|\varphi\rangle$ may be written as

$$|\varphi\rangle = \sum_{i=1}^N a_i |g_i\rangle, \quad (35)$$

where the coefficients a_i are given by simple algebraic relations in terms of α_i and β_i [30]. The Schwinger-Lanczos approach is iterative and does not require inversion of any matrix. The number N here denotes the total number of Lanczos steps. The number of Lanczos steps needed for the method to converge depends on the "strength" of the operator F .

In the specific case of the $e + \text{HBr}$ collision complex, as in $e + \text{HCl}$, the nonlocal potential F is strong and the convergence of the Schwinger-Lanczos method with respect to N relatively slow. In the present work we have implemented a modification of the method which exhibits improved convergence properties [45]. We introduce a local approximation F_{loc} to the nonlocal operator F and employ the Schwinger-Lanczos procedure for the difference potential $F - F_{\text{loc}}$.

The local approximation F_{loc} is introduced as follows. Generally F acts on a wave function φ as

$$\langle R|F|\varphi\rangle = \int F(R, R'; E) \varphi(R') dR'. \quad (36)$$

Let us expand the wave function $\varphi(R')$ into a Taylor series around a point R . Then

$$\begin{aligned} \langle R|F|\varphi\rangle &= \int F(R, R'; E) [\varphi(R) + \varphi'(R)(R - R') + \frac{1}{2}\varphi''(R) \\ &\quad \times (R' - R)^2 + \dots] dR'. \end{aligned} \quad (37)$$

If the wave function $\varphi(R)$ does not change very rapidly with R the higher terms in Eq. (37) can be neglected and $F|\varphi\rangle$ can be approximated by [46]

$$\langle R|F|\varphi\rangle \approx \int F(R, R'; E) dR' \varphi(R) = F_{\text{loc}}(R, E) \varphi(R). \quad (38)$$

$F_{\text{loc}}(R, E)$ here is a local complex energy-dependent potential. It is also possible to include higher terms in Eq. (37) but for our purposes this is not necessary.

Having obtained the local complex potential F_{loc} we can write the LS equation (27) as

$$|\varphi\rangle = |u\rangle + G_d F_{\text{loc}} |\varphi\rangle + G_d (F - F_{\text{loc}}) |\varphi\rangle. \quad (39)$$

Applying again the two-potential formula, Eq. (27) is rewritten as

$$|\varphi\rangle = |v\rangle + G_d (F - F_{\text{loc}}) |\varphi\rangle, \quad (40)$$

where

$$|v\rangle = (1 - G_d F_{\text{loc}})^{-1} |u\rangle \quad (41)$$

and

$$G = (1 - G_d F_{\text{loc}})^{-1} G_d. \quad (42)$$

The Schwinger-Lanczos method is then applied, as described above, to Eq. (40).

To generate the nonlocal operator F according to Eqs. (2)–(4), a set of vibrational states $|\chi_v\rangle$ is constructed by diagonalizing the matrix representation of H_0 in a suitable basis of square-integrable functions. A discrete variable approach (DVR) is employed for this purpose. Approximately 100 DVR functions are required to get an accurate representation of the target wave functions (for details see [45]). The summations in Eqs. (3) and (4) are truncated at v_{max} which depends on the incident electron energy. It has been checked that $\Gamma(R, E)$ and $\Delta(R, E)$ thus obtained are completely converged both with respect to the DVR grid as well as the summation over target vibrational levels. This construction of $\Gamma(R, E)$ and the solution of the LS equation via the Schwinger-Lanczos approach are completely general procedures and do not depend on special analytic forms of the potentials $V_0(R)$ and $V_d(R)$, as has been the case in some previous treatments [17].

It has been found that the introduction of F_{loc} can substantially reduce the number of recursion steps needed for convergence of the Schwinger-Lanczos procedure [45]. This is particularly true in the energy range of the threshold peaks, where the computation of fully converged cross sections may require very high N .

V. RESULTS

A. HBr

Integral VE cross sections for the $0 \rightarrow 1$, $0 \rightarrow 2$, and $0 \rightarrow 3$ channels are shown in Fig. 3. The $v = 0 \rightarrow 1$ cross section exhibits an intense and narrow threshold peak as well as a shape resonance feature near 1 eV impact energy, in qualitative agreement with the experimental data of Rohr [10]. The absolute value of the calculated integral $0 \rightarrow 1$ cross section at the resonance peak near 1 eV impact energy is smaller by a factor of about 5 than the value reported by Rohr. This is shown in Fig. 4(a).

The intensity of the threshold peak relative to the shape resonance peak is larger in the present calculation than in Rohr's experiment. It should be noted, however, that the intensity and width of the threshold peak are very sensitive to changes of the input data of the model. Because of the limited accuracy of the *ab initio* data and the limitations of the fitting procedure, there is some uncertainty in the model parameters and the present results should therefore not be considered as a reliable prediction of the intensity and shape of the threshold peak. On the experimental side, the determination of accurate cross sections very close to threshold is notoriously difficult, see, e.g., the discussion in Ref. [21]. The determination of the precise intensity and width of the threshold peak in the $0 \rightarrow 1$ channel of HBr is thus still an open problem. The present calculations strongly support, however, the existence of a pronounced threshold peak in agreement with Rohr's experiment.

We find no intense threshold peaks in the $v = 0 \rightarrow 2$ and higher channels. This confirms the conclusion of Azria *et al.* [47] that the threshold peaks reported by Rohr [10] for the higher channels are due to Br^- ions.

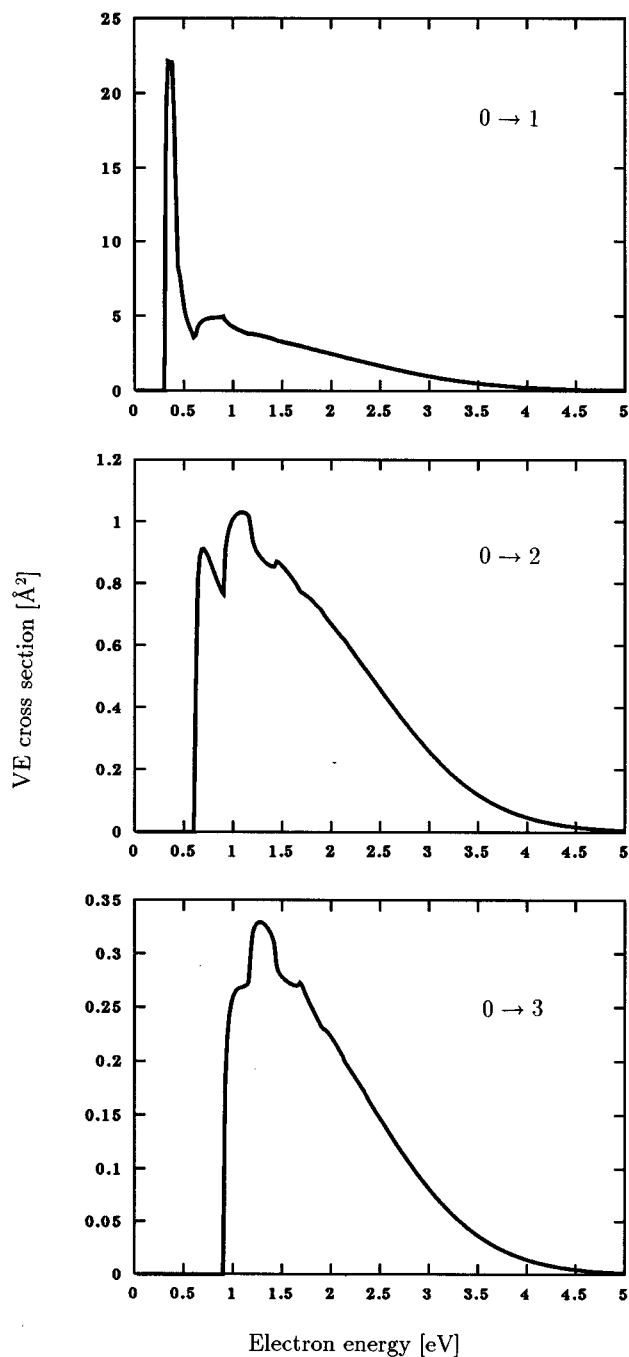


FIG. 3. Integral VE cross section for the $v=0 \rightarrow 1$, $v=0 \rightarrow 2$, and $v=0 \rightarrow 3$ channels.

The present $v=0 \rightarrow 1$ cross section is in qualitative agreement with the calculation of Fandreyer *et al.* [24], although we find a narrower threshold peak and our shape resonance feature is located at lower energy. The two calculations are compared in Fig. 4(b); the solid line represents our results, the dashed line that of Fandreyer *et al.* [24]. For the $v=0 \rightarrow 2$ channel, on the other hand, we find a completely different shape of the excitation function than the calculation of Fandreyer *et al.* Considering the excellent agreement of the fixed-nuclei eigenphase sum of the present model with the data of Fandreyer *et al.* (see Fig. 1), it appears probable that the nonadiabatic treatment of the vibrational motion in

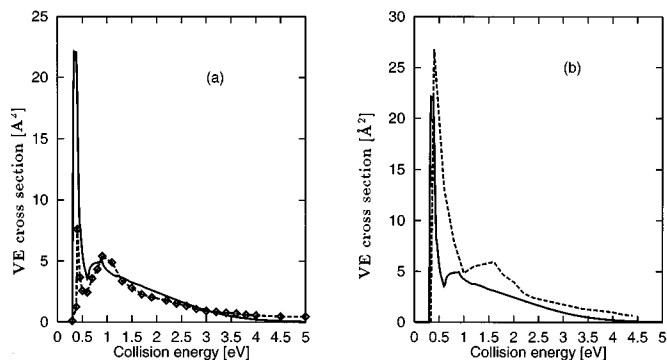


FIG. 4. (a) Integral VE cross section for the $v=0 \rightarrow 1$ channel. The solid line shows results of the present calculation whereas the dashed line with diamonds shows the experimental results of Rohr [10] scaled by the factor 0.2. (b) Integral VE cross section for the $v=0 \rightarrow 1$ channel. The solid line shows results of the present calculation whereas the dashed line shows that of Fandreyer *et al.* [24].

[24] has not been fully converged. Whether this reflects a fundamental limitation of the *R*-matrix approach of Ref. [24] or merely a technical problem of the calculation is beyond our judgment.

Although the absolute values of our VE cross sections differ from the values reported by Rohr [10], it appears that the relative values of the calculated cross sections for different VE channels are in very good agreement with the experimental data. Since the absolute values of the cross sections in the threshold region are less reliable than that in the resonance region (1.0 – 1.5 eV) we compare their values at energies at which they attain their maxima in this region. The ratios of VE cross sections calculated in this way are shown in Table I. The agreement with the experimental values [10] is very good.

The calculated DA cross section is compared with experiment in Fig. 5. The solid line represents our calculation, while the dashed line gives the relative experimental results of Abouaf and Teillet-Billy [48], normalized at the peak value of the cross section to the present data. The shape of the calculated DA profile is in good agreement with experiment (considering that the experiment contains contributions from rotationally hot molecules) [48]. The characteristic Wigner cusps at the openings of VE channels are very well reproduced by the calculation. The calculated peak value of 4.5 \AA^2 is considerably larger than in HCl, in agreement with experimental estimates [Christophorou, Compton, and Dick-

TABLE I. Ratios of VE cross sections.

σ_a / σ_b	Experiment	Calculation
$0 \rightarrow 2 / 0 \rightarrow 1$	0.2	0.21
$0 \rightarrow 3 / 0 \rightarrow 1$	0.05	0.07
$0 \rightarrow 4 / 0 \rightarrow 1$	0.02	0.02
$0 \rightarrow 5 / 0 \rightarrow 1$	0.006	0.009
$0 \rightarrow 3 / 0 \rightarrow 2$	0.24	0.32
$0 \rightarrow 4 / 0 \rightarrow 3$	0.33	0.36
$0 \rightarrow 5 / 0 \rightarrow 4$	0.37	0.39

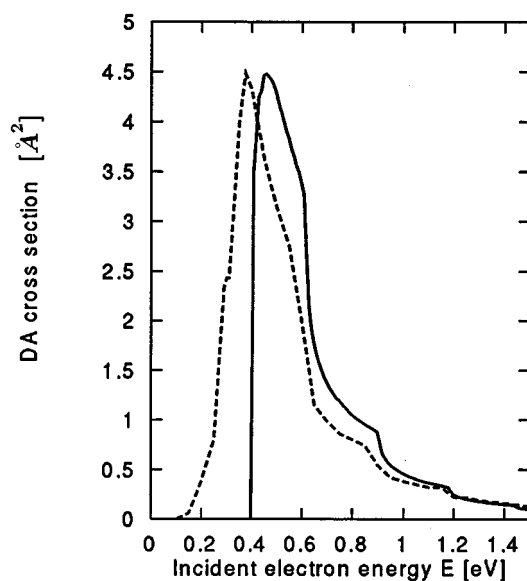


FIG. 5. DA cross section from the ground vibrational state. Solid line— present calculation, dashed line—experimental results of Abouaf and Teillet-Billy [48] normalized at the peak value of the cross section.

son [49] report two peak values of the DA cross section: 4.0 \AA^2 (folded) and the probably more reliable unfolded value 2.7 \AA^2 [49]. The enhanced DA cross section compared with HCl reflects the longer lifetime of the $^2\Sigma^+$ shape resonance of HBr.

VE and deexcitation cross sections of hydrogen halides are of relevance for the modeling of gas laser plasmas [4,5]. We have therefore also computed inelastic and superelastic cross sections for HBr molecules in the vibrationally excited levels $v=1,2,3$. In Fig. 6 we show the cross sections for the transitions $1 \rightarrow 0$, $1 \rightarrow 2$, and $1 \rightarrow 3$. Because of the excitation of the target molecule, the vibrational thresholds are shifted to lower energies. The $1 \rightarrow 2$ VE cross section exhibits a threshold peak which is, however, lower and broader than the corresponding peak in the $0 \rightarrow 1$ transition. We do not find threshold peaks in the higher transitions $1 \rightarrow v$, $v=3,4,5, \dots$

The calculated VE and deexcitation cross sections for the second excited vibrational state of the target molecule are shown in Fig. 7. The threshold structures are reduced in intensity and it is hardly possible to speak of threshold peaks in the transitions $2 \rightarrow 3$, $2 \rightarrow 4$, etc.

In Fig. 8 the calculated DA cross sections are shown for the three initial vibrational states $v_{\text{in}}=0, 1$, and 2 . The calculation confirms the results known from the experiment on HCl [50] that even a small fraction of vibrationally excited molecules in the target gas can considerably increase the DA cross section. Here, for instance, the DA cross section for the first excited state reaches a value higher than 60 \AA^2 . For $v=2$, the DA process becomes exothermic and the DA cross section diverges for $E \rightarrow 0$.

The high efficiency and accuracy of our approach allow us to investigate very detailed structures in cross sections. One such structure is observed in the elastic and the $0 \rightarrow 1$ VE cross sections in the vicinity of the DA threshold. The $0 \rightarrow 1$ VE cross section exhibits a very deep minimum just

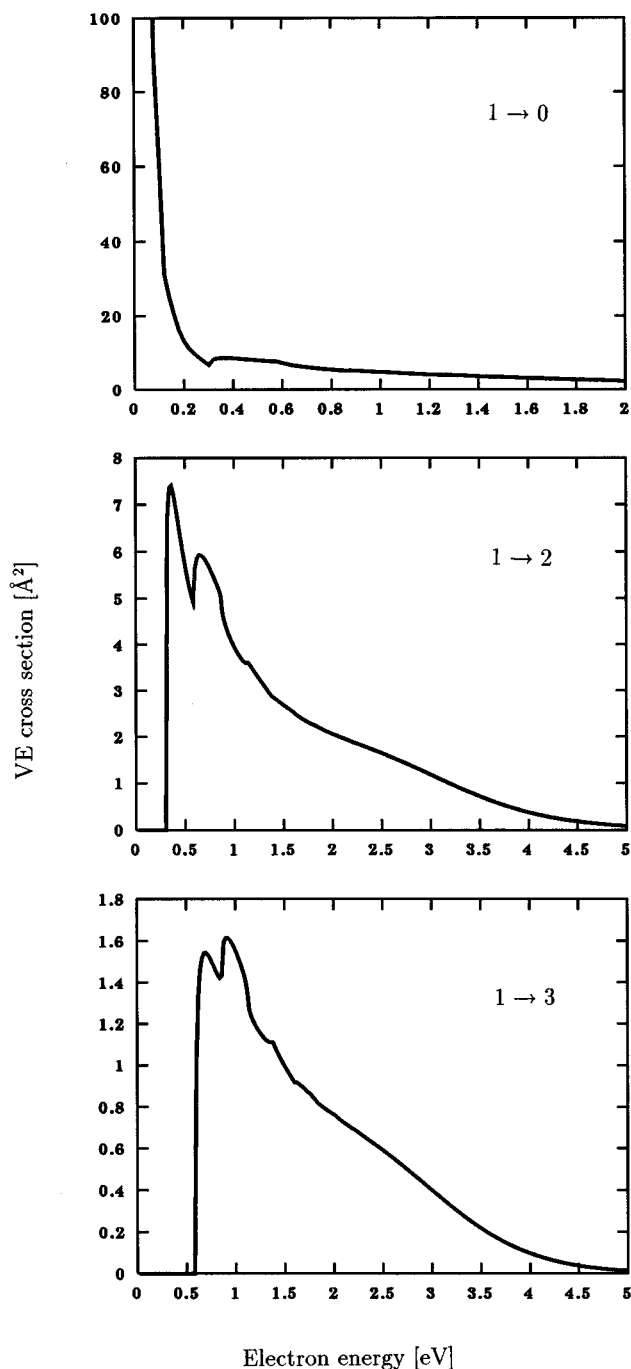


FIG. 6. Integral VE cross sections for the $v=1 \rightarrow 0$, $v=1 \rightarrow 2$, and $v=1 \rightarrow 3$ channels for vibrationally excited HBr molecules ($v_{\text{in}}=1$).

below the DA threshold. Rapid changes are observed at the same energy in the resonant part of the elastic cross section, as shown in Fig. 9. This narrow resonance feature reflects a quasibound level in the shallow well of the HBr^- potential at large internuclear distances (cf. Fig. 2). The accurate calculation of this feature is a demanding task as far as the solution of the scattering equations is concerned. Moreover, the position and width of this window resonance are very sensitive to the PE functions and the discrete-continuum coupling function at large internuclear distances. The experimental observation of such resonance features would thus

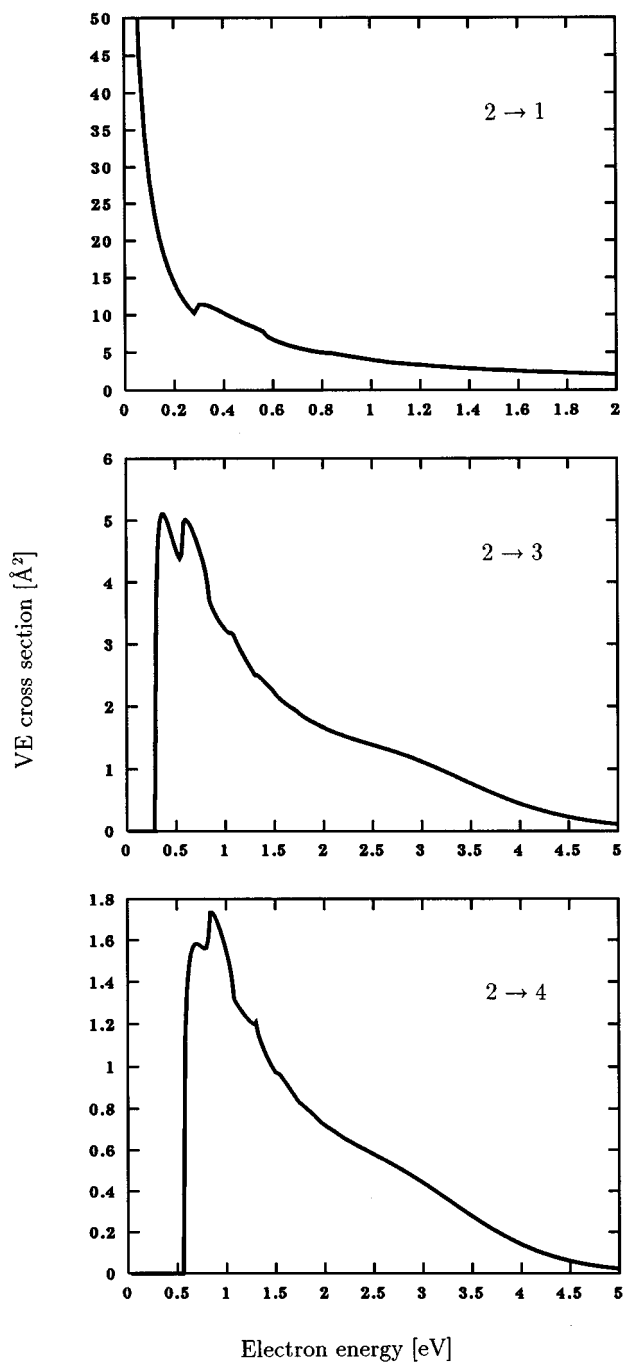


FIG. 7. The same as in Fig. 6 but $v_{in}=2$.

provide very detailed information on the HBr^- system.

The present model for electron-HBr scattering does not predict the oscillatory fine structure below the DA threshold observed in the $0 \rightarrow 1$ and $0 \rightarrow 2$ excitation functions of the $e + \text{HCl}$ system [9,21]. However, the accuracy of the *ab initio* data [24] and the accuracy of the present fitting procedure are not sufficient to allow definitive predictions of fine details, and such structures might exist. In any case, the present calculations indicate that the measurement of VE excitation functions of HBr with high sensitivity and good energy resolution would be a very worthwhile undertaking.

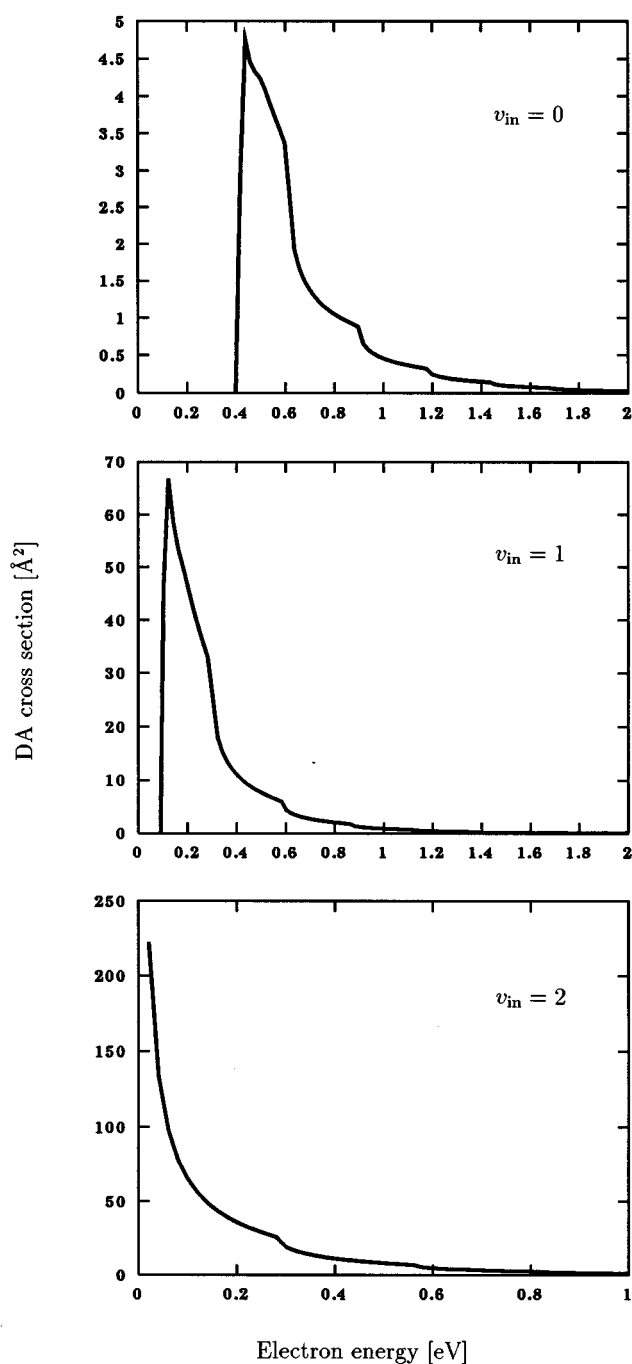


FIG. 8. DA cross sections for three initial vibrational states of HBr ($v_{in}=0, 1, \text{ and } 2$).

B. DBr

In order to investigate the isotope effect which is known to be pronounced in DA to hydrogen halides [50,51] we have calculated VE and DA cross sections also for DBr molecules. The VE cross sections for the DBr molecule in the ground vibrational state are shown in Fig. 10. The corresponding DA cross sections are shown in Fig. 11. In contrast to the HBr case we observe here a pronounced threshold peak also in the $0 \rightarrow 2$ channel. Threshold peaks are again absent in the higher transitions. The value of the $0 \rightarrow 1$ VE cross section at the peak is lower than that for HBr, reaching only 12\AA^2 .

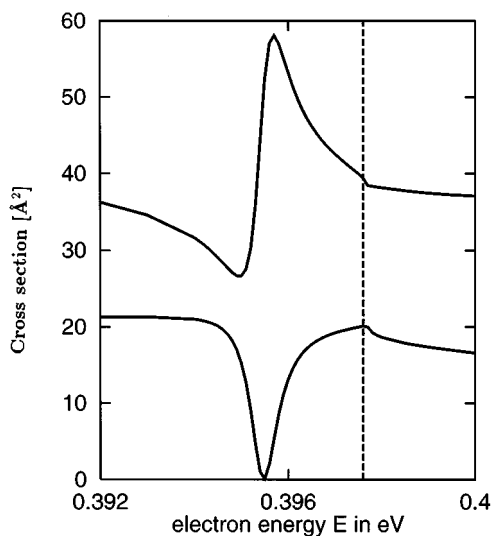


FIG. 9. Structure in VE cross sections ($0 \rightarrow 0$ —upper line and $0 \rightarrow 1$ —lower line) of HBr in the vicinity of the DA threshold.

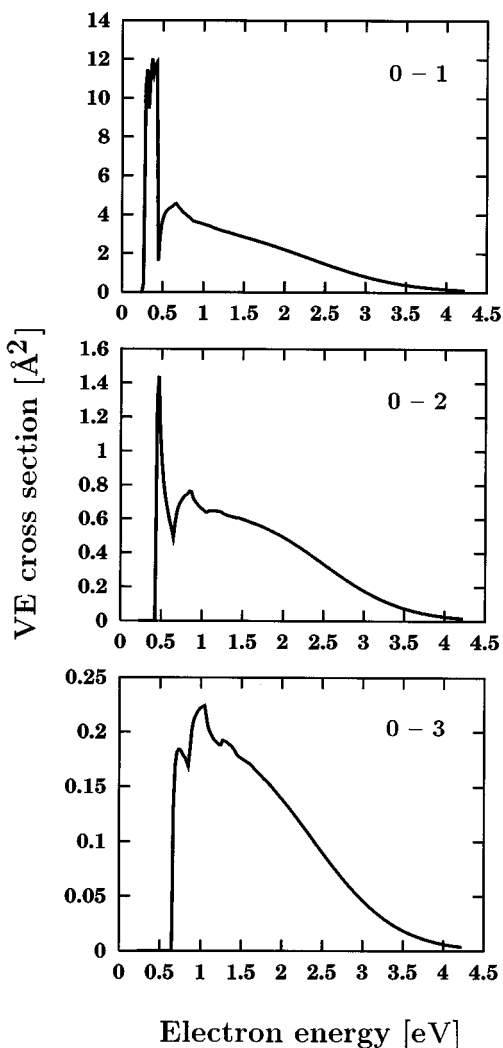


FIG. 10. Integral VE cross sections for DBr: $0 \rightarrow 1$, $0 \rightarrow 2$, and $0 \rightarrow 3$ channels.

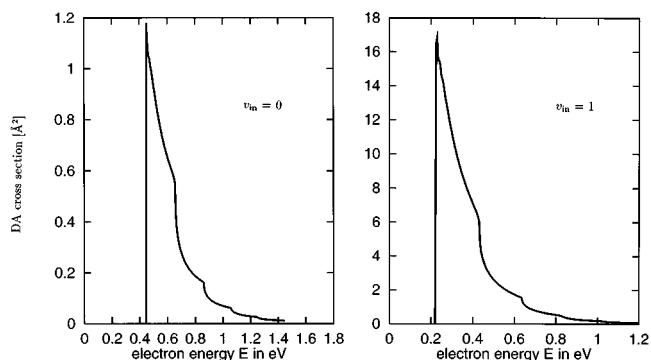


FIG. 11. DA cross sections for two initial vibrational states of DBr ($v_{in}=0$ and 1).

The cross section of dissociative electron attachment to DBr is considerably lower than that of HBr. The two DA cross sections are compared in Fig. 12. The dashed line represents the DA cross section in HBr, whereas the solid line gives the DA cross section in DBr. The isotope effect is very pronounced in this case (a factor of ≈ 4.5), but less pronounced than in HCl, where a factor of ≈ 10 is predicted by theory [17]. This reflects again the longer lifetime of the DBr^- collision complex compared to DCl^- .

VI. CONCLUSION

In this paper we have reported on extensive calculations of the vibrational-excitation cross sections and of dissociative attachment cross sections for low-energy electrons colliding with HBr and DBr molecules. The nonlocal resonance model which has been developed for the description of VE and DA in electron-HCl collisions [17,18,25] has been used. The parameters of the model were obtained by fitting the *ab initio* fixed-nuclei scattering data of Fandreyer *et al.* [24]. The nuclear scattering dynamics in the complex and nonlocal effective potential of the resonance state has been treated in

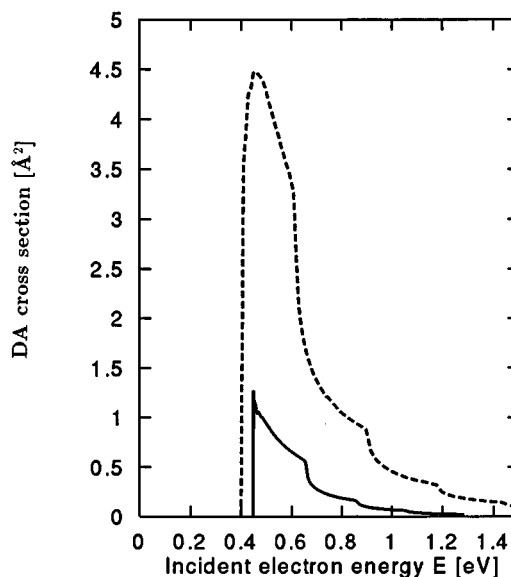


FIG. 12. DA cross sections for DBr—solid line. The dashed line shows the DA cross section for HBr.

the Schwinger-Lanczos approach [29–31].

The results of the present calculations are in good agreement with experiment, as far as data are available. The absolute values of the calculated $0 \rightarrow v$ VE cross sections are significantly smaller than the values reported by Rohr [10]. The fact that the relative cross sections for different channels agree very well with Rohr's data strongly indicates that the absolute normalization of the experimental data [10] should be reconsidered. The calculations confirm the existence of a pronounced threshold peak in the $0 \rightarrow 1$ channel of HBr, in qualitative agreement with the measurement of Rohr [10], and the absence of threshold peaks in higher channels, as suggested by Azria *et al.* [47]. The calculated DA cross section appears to be in excellent agreement with the measurement of Abouaf and Teillet-Billy [the apparent shift of the experimental profile to lower energies (see Fig. 5) arises from thermal rotational excitation of the target molecules,

which is not considered in the calculation]. We have made predictions of various VE and deexcitation cross sections for vibrationally excited target molecules, as well as of HBr-DBr isotope effect. These data could potentially be useful for the modeling of discharges containing HBr or DBr molecules.

The predictions of the present work rely on the *ab initio* fixed-nuclei scattering data of [24] and depend on the validity of the fitting procedure, that is, the adequacy of the non-local resonance model. More extensive and more accurate experimental data are needed to either verify these predictions or to reveal the need of improved calculations.

ACKNOWLEDGMENT

This work has been supported by the Deutsche Forschungsgemeinschaft.

-
- [1] K. Rohr and F. Linder, *J. Phys. B* **8**, L200 (1975).
 [2] K. Rohr and F. Linder, *J. Phys. B* **9**, 2521 (1976).
 [3] R. Abouaf and D. Teillet-Billy, *J. Phys. B* **10**, 2261 (1977).
 [4] *Applied Atomic Collision Physics*, edited by E. W. McDaniel and W. L. Nigham, Gas Lasers Vol. 3 (Academic Press, New York, 1982).
 [5] T. Hammer and W. Böttcher, *Appl. Phys. B* **48**, 73 (1989).
 [6] G. Knoth, M. Rädle, H. Ehrhardt, and K. Jung, *Europhys. Lett.* **4**, 805 (1987).
 [7] G. Knoth, M. Gote, M. Rädle, K. Jung, and H. Ehrhardt, *Phys. Rev. Lett.* **62**, 1735 (1989).
 [8] G. Knoth, M. Rädle, M. Gote, H. Ehrhardt, and K. Jung, *J. Phys. B* **22**, 299 (1989); **22**, 1455 (1989).
 [9] O. Schafer and M. Allan, *J. Phys. B* **24**, 3069 (1991).
 [10] K. Rohr, *J. Phys. B* **11**, 1849 (1978).
 [11] H. T. Thümmel, R. K. Nesbet, and S. D. Peyerimhoff, *J. Phys. B* **26**, 1233 (1993).
 [12] L. A. Morgan and P. G. Burke, *J. Phys. B* **21**, 2091 (1988).
 [13] I. I. Fabrikant, S. A. Kalin, and A. K. Kazansky, *J. Phys. B* **25**, 2885 (1992).
 [14] H. Feshbach, *Ann. Phys. (N.Y.)* **19**, 287 (1962).
 [15] I. I. Fabrikant, *Comments At. Mol. Phys.* **24**, 37 (1990).
 [16] I. I. Fabrikant, S. A. Kalin, and A. K. Kazansky, *J. Chem. Phys.* **95**, 4966 (1991).
 [17] W. Domcke and C. Mündel, *J. Phys. B* **18**, 4491 (1985).
 [18] P. L. Gertitschke and W. Domcke, *Z. Phys. D* **31**, 171 (1994).
 [19] D. Teillet-Billy and J. P. Gauyacq, *J. Phys. B* **17**, 4041 (1984).
 [20] L. A. Morgan, P. G. Burke, and C. J. Gillan, *J. Phys. B* **23**, 90 (1990).
 [21] S. Cvejanović, in *Proceedings of the 18th International Conference on the Physics of Electronic and Atomic Collisions, Aarhus, 1993, Abstracts of Contributed Papers*, edited by T. Andersen, B. Fastrup, F. Folkmann, and H. Knudsen (Aarhus University, Aarhus, Denmark, 1993).
 [22] M. A. Morrison, *Adv. At. Mol. Phys.* **24**, 51 (1988).
 [23] W. Domcke, *Phys. Rep.* **208**, 97 (1991).
 [24] R. Fandreyer, P. G. Burke, L. A. Morgan, and C. J. Gillan, *J. Phys. B* **26**, 3625 (1993).
 [25] W. Domcke and L. S. Cederbaum, *J. Phys. B* **14**, 149 (1981).
 [26] D. A. Chapman, K. Balasubramanian, and S. H. Lin, *Phys. Rev. A* **38**, 6098 (1988).
 [27] C. Mündel and W. Domcke, *J. Phys. B* **17**, 3593 (1984).
 [28] V. Pless, B. N. Nestmann, and S. D. Peyerimhoff, *J. Phys. B* **25**, 4649 (1992).
 [29] J. Horáček and T. Sasakawa, *Phys. Rev. A* **28**, 2151 (1983); *A* **30**, 2274 (1984); *Phys. Rev. C* **32**, 70 (1985).
 [30] H.-D. Meyer, J. Horáček, and L. S. Cederbaum, *Phys. Rev. A* **43**, 3587 (1991).
 [31] J. Horáček, *J. Phys. B* **28**, 1585 (1995).
 [32] J. Horáček and W. Domcke, *Chem. Phys. Lett.* **234**, 304 (1995).
 [33] J. C. Y. Chen, *Phys. Rev.* **148**, 66 (1966).
 [34] T. F. O'Malley, *Phys. Rev.* **150**, 14 (1966).
 [35] J. N. Bardsley, *J. Phys. B* **1**, 349 (1968).
 [36] H. Nakamura, *J. Phys. Soc. Jpn.* **31**, 574 (1971).
 [37] F. Fiquet-Fayard, *J. Phys. B* **7**, 810 (1974).
 [38] T. F. O'Malley, *Phys. Rev.* **137**, A1668 (1965).
 [39] G. Herzberg, *Molecular Spectra and Molecular Structure I. Spectra of Diatomic Molecules* (Van Nostrand, New York, 1950).
 [40] C. W. Clark, *Phys. Rev. A* **30**, 750 (1984).
 [41] F. A. van Dijk and A. Dymanus, *Chem. Phys. Lett.* **5**, 387 (1970).
 [42] H. Hotop and W. C. Lineberger, *J. Phys. Chem. Ref. Data* **4**, 539 (1975).
 [43] D. T. Birtwistle and A. Herzenberg, *J. Phys. B* **4**, 53 (1971).
 [44] A. U. Hazi, T. N. Rescigno and M. Kurilla, *Phys. Rev. A* **23**, 1089 (1981).
 [45] J. Horáček, F. Gemperle, and H.-D. Meyer (unpublished).
 [46] B. H. Bransden, M. R. C. McDowell, C. J. Noble, and T. Scott, *J. Phys. B* **9**, 1301 (1976).
 [47] R. Azria, Y. Le Coat, and J. P. Guillotin, *J. Phys. B* **13**, L505 (1980).
 [48] R. Abouaf and D. Teillet-Billy, *Chem. Phys. Lett.* **73**, 106 (1980).
 [49] L. G. Christophorou, R. N. Compton, and H. W. Dickson, *J. Chem. Phys.* **48**, 1949 (1968).
 [50] M. Allan and S. F. Wong, *J. Chem. Phys.* **74**, 1687 (1981).
 [51] R. Azria, L. Roussier, R. Paineau, and M. Tronc, *Rev. Phys. Appl.* **9**, 469 (1974).